Unravelling the growth mechanism of (3,1) graphene nanoribbons on a Cu(111) surface

Elie Geagea,[a] Judicael Jeannoutot, [a] Louise Morgenthaler, [a] Simon Lamare, [a] Alain Rochefort, [b] Frank Palmino [a] and Frédéric Chérioux [a,*]

The growth of graphene nanoribbons has been widely investigated on metal surfaces in ultrahigh vacuum. Here, we re-investigate the growth of graphene nanoribbons obtained by thermal annealing of 9,9'-bianthryl derivatives on a Cu(111) surface by using scanning tunnelling microscopy. On the basis of our results, we propose to complete the reaction mechanism commonly accepted in the literature by adding a hydrogen atom transfer from 2,2'-positions to 10,10'-positions as a key-step in the formation of (3,1)-graphene nanoribbons on a Cu(111) surface.

Graphene nanoribbons (GNRs) are 1D graphene stripes which are widely investigated due to their remarkable electronic properties compared to 2D graphene.[1] To achieve GNRs with well-defined edge configuration and width, and accordingly control these electronic properties, growth was from wisely-chosen molecular building-blocks was optimized thanks to atomic-scale characterizations using scanning probe microscopies under ultra-high vacuum (UHV).[2,3,4,5,6] Among all accessible molecular building blocks for the on-surface synthesis of GNRs, 10,10'-dihalogenated-9,9'-bianthryl derivatives [2] and 9,9'-bianthryl[4,5,6] are the two most commonly used. In the case of 10,10'-dihalogenated-9,9'-bianthryl derivatives, the formation of a large variety of GNRs is based on a thermally-induced Ullmann cross-coupling followed by a cyclodehydrogenation on different kinds of coinage metal surfaces.[2]

Non-halogenated 9,9'-bianthryl derivatives lead to chiral (3,1)-GNRs, but only on a copper surfaces. [4,5,6] After few controversies,[7] the currently accepted reactional mechanism for the growth of chiral (3,1)-GNRs on a Cu(111) surface is based on a first thermal annealing leading to a protopolymer thanks to on surface-assisted generation of a 2,2'-diradical species. Then, further heating gives the targeted chiral (3,1)-GNR as result of ring-closure driven by a cyclodehydrogenation (Scheme 1a). Most of the reaction intermediates involved in this mechanism have been observed.[4,5,6]

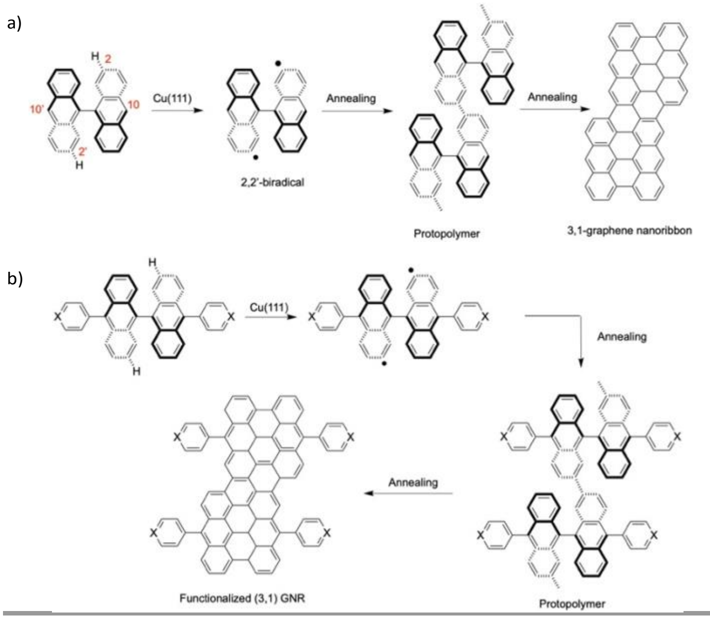

Scheme 1: a) Reaction mechanism accepted for the synthesis of chiral (3,1) GNR on a Cu(111) surface by using 9,9'-bianthryl as precursor. The key-step is the surface-assisted formation of 2,2'-biradical specie which points to the surface. b) Possible chemical pathway for the formation of laterally functionalized (3,1) GNRs based on the reaction mechanism described in a). Dashed-bonds are pointing to the surface while bold bonds are pointing out the surface.

A corollary of this reaction mechanism[6] is the opportunity to synthesis functional (3,1) GNRs by introducing functional groups on the 10,10' positions of the starting building blocks (Scheme 1b). Despite its potential for producing a large variety of GNRs with tailored properties, no implementation of this strategy has been reported so far to our knowledge. In this article, we investigate the growth of laterally functionalized (3,1) chiral GNRs by thermal-induced reaction of 10,10'-di(aryl)-9,9'-bianthryl on a Cu(111) surface in UHV by scanning tunnelling microscopy (STM). We find that the growth of GNRs is not possible when the 10,10' positions of the starting building blocks are substituted by aryl groups. Therefore, we revisit the commonly accepted reaction mechanism accounting for the growth of (3,1) GNR on a Cu(111)-surface to explain this phenomenon.

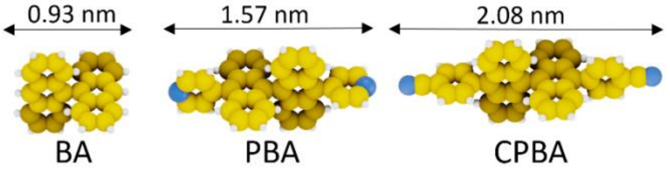

Fig. 1: CPK models of the 9,9'-bianthryl (BA), the 10,10'-di(4''-pyridyl)9,9'-bianthryl (PBA) and the 10,10'-di(4''-cyanophenyl)9,9'-bianthryl (CPBA) molecules respectively.

We selected the widely-investigated of 9,9'-bianthryl (BA) as a model compound to secure our experimental procedure for the growth of chiral (3,1) GNRs on Cu(111). We synthesized two other molecules, 10,10'-di(4''-pyridyl)9,9'-bianthryl (PBA) and 10,10'-di(4''-cyanophenyl)9,9'-bianthryl (CPBA) respectively, that contain two aryl groups covalently bounded to 10 and 10' positions (Fig. 1 and Fig S1-2 of ESI). We chose cyano phenyl and pyridyl groups as aryl group because they promote the formation of supramolecular on various kinds of surface even at room temperature.[8] The synthesis of molecules and surface preparation are fully described in electronic supplementary information. The molecules were deposited by thermal sublimation under UHV on a Cu(111) substrate maintained at room temperature. As revealed in STM images recorded at 110 K (Fig S3-4 of ESI), no isolated molecule was observed but only large extended 2D islands, each one being constituted by the periodic arrangement of several bright protrusions. The repeat unit pattern of each STM image is in accordance with the distance between the edges of the topmost carbon ring of each of the two anthracenyl subunits of molecules (Fig S4 of ESI). Then, we investigated the chemical transformations of these supramolecular networks induced by thermal annealing. Each supramolecular network was exposed to subsequent thermal annealing up to 673 K from 1h to 4h.

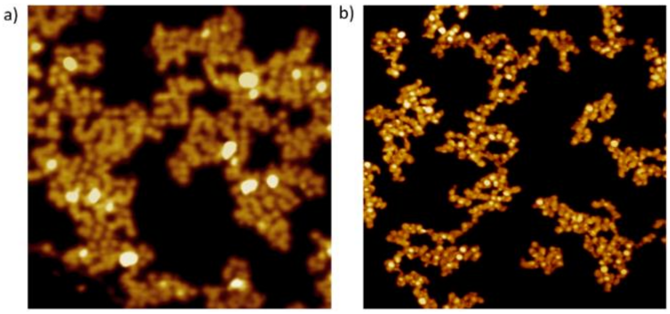

Fig. 2: STM images of linear structures formed after subsequent annealing of BA supramolecular network up to 673 K on Cu(111) surface (V_s=-1.4 V, I_t=10 pA, 30x30nm. On the right, zoomed STM image corresponding to the blue dashed square (4x4 nm^2) of linear GNRs with superimposed structural model.

In the case of BA molecules, thermal annealing (673 K) led to the formation of clearly linear nanostructures with lengths up to 17.3 nm (Fig. 2 and Fig. S5 of ESI). A zoom of this STM image (area outlined by blue dashed square in Fig. 2) reveals continuous nanolines, with a uniform apparent height, and clearly seamless. This image is similar to those reported in the literature for chiral (3,1) GNRs.[4,5,6] This experiment confirms that our experimental procedure leads to the formation of (3,1) GNRs on Cu(111).

In the case of PBA and CPBA supramolecular networks, the same thermal annealing (673 K) led to disordered nanostructures (Fig. 3). The STM images show apparently random nanostructures, without any linear feature corresponding to targeted GNRs.

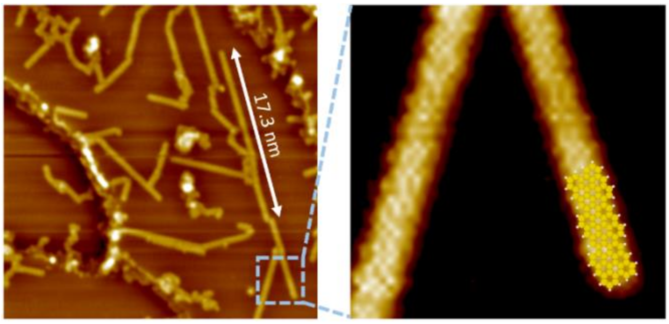

Fig. 3: STM images of disordered features obtained after subsequent annealing of PBA and CPBA supramolecular networks up to 673 K on a Cu(111) surface, respectively. a) PBA (V_s =1.8 V, I_t =10 pA, 40x40 nm^2) and b) CPBA (V_s =-1.2 V, I_t =10 pA, 70x70 nm^2)

We made different thermal annealing, with temperature from 400 to 673 K. However, we never observed linear nanostructures corresponding to functionalized (3,1) GNRs, but only disordered features. This result is very surprising because, according to the reported reaction mechanism,[4,5,6] the presence of aryl substituents at the 10 and 10’ positions should be in agreement with the formation of corresponding (3,1) GNRs (Scheme 1b). Moreover, STM images of the starting supramolecular networks suggest that the cyanophenyl or the pyridyl substituents are not pointing to the surface but they are still in the plane of the surface because they are involved in the molecule-molecule interactions (Fig. S3c-d of ESI). As usual, one ring per anthracenyl arm is still pointing to the surface, as observed for BA molecules (Fig. S3b of ESI), indicating that the 2,2’-biradical could be stabilized by the surface if it is (previously) formed.

Therefore, as no (3,1) GNR was observed by using PBA and CPBA as building blocks, we conclude that the surface-induced cleavage of C-H of 2 and 2’ positions is not possible by annealing on a Cu(111). Because of the canonical forms of BA governing the reactivity of fused six-membered aromatic rings,[9] we assume that the thermally-induced cleavage of C-H bonds is only possible on 10 and 10’ positions, even on a Cu(111) surface, to give biradical species (Scheme 2). Then, a hydrogen atom transfer[10] from the 2,2’-positions to the 10,10’-positions occurs, leading to the formation of the 2,2’-biradical. To assume this hypothesis, we performed DFT calculations. They indicate that 2,2’-biradical is more stable than 10,10’-biradical by around 290meV on a Cu(111) surface while in the vacuum the 10,10’-biradical is more stable by around 40meV. In addition, the DFT calculations shows that the involved stabilizing surface-molecule interaction originates from the radicals on 2,2’-positions which are pointing to the surface (Fig S6 and S7 of ESI). This hypothesis also justifies why only 2,2’-biradicals are observed by nc-AFM while 10,10’-biradicals are never observed.[6] Finally, the 2,2’-biradical leads to a protopolymer and then, to a (3,1) GNR by a second annealing (Scheme 2). On the contrary, if 10 and 10’ positions are substituted by aryl groups, C-H bond on 2,2’-positions are not cleaved by soft annealing (below 500K) to give corresponding radicals even with the assistance of the underlying surface. In this case, a stronger annealing (673 K) is necessary to induce the activation of C-H leading to the growth of very disordered features on the reactive Cu(111) surface due to cyclodehydrogenation and non-directed fusing of aromatic ring.[11]

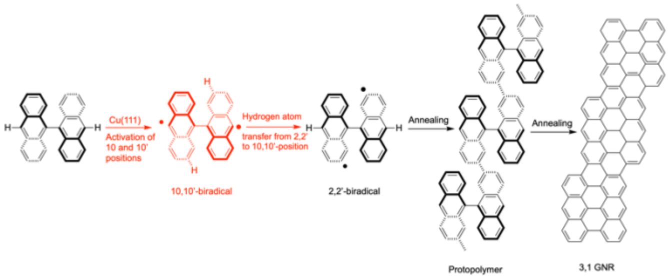

Scheme 2: Completed reaction mechanism for the growth of (3,1) GNR induced by a two-step annealing of BA molecules on a Cu(111) surface. The formation of 10,10’-biradical (in red), followed by radical transposition, is added as initial step.

In conclusion, we have re-investigated the reaction mechanism of growth of (3,1) GNRs on a Cu(111) surface. On the basis of our experimental observations, we propose to complete the reported reaction mechanism by adding an initial step. We state that the first step consists in the C-H bond cleavage of the 10,10’ positions, with respect to the canonical forms, followed by a hydrogen atom transfer from the 2,2’-positions to the 10,10’-positions (Scheme 2). Then, the 2,2’-biradical follows the previously accepted reaction mechanism. This new reaction mechanism paves the way to new possibilities for on-surface assisted synthesis of functional nanostructures.

The authors acknowledge the financial support from the French National Research Agency through contract OVATION (ANR-19-CE09-0020) and from the Pays de Montbéliard Agglomération. The authors thank Dr S. Benchabane (FEMTO-ST) and Dr J. Coraux (Neel, Grenoble, France) for fruitful discussions.

Author Contributions

L.M. and S.L. synthetised all molecules. E.G., J.J. and F.P. performed STM experiments. E.G., F.P and F.C. wrote the manuscript with inputs from all authors.

Conflicts of interest

There are no conflicts to declare.

Notes and references

1 D. J. Rizzo, G. Veber, T. Cao, C. Bronner, T. Chen, F. Zhao, H. Rodriguez, S. G. Louie, M. F. Crommie and F. R. Fischer, *Nature*, 2018, **560**, 204; O. Gröning, S. Wang, X. Yao, C. A. Pignedoli, G. Borin Barin, C. Daniels, A. Cupo, V. Meunier, X. Feng, A. Narita, K. Mullen, P. Ruffieux, R. Fasel, *Nature*, 2018, **560**, 209.

2 J. Caï, P. Ruffieux, R. Jaafar, M. Bieri, T. Braun, S. Blankeburg, M. Muoth, A. P. Seitsonen, M. Saleh, X. Feng, K. Mullen, R. Fasel, *Nature*, 2010, **466**, 470; D. G. de Oteyza, A. Garcia-Lekue, M. Vilas-Varela, N. Merino-Diez, E. Carbonell-Sanroma, M. Corso, G. Vasseur, C. Rogero, E. Guitan, J. I. Pascual, J. E. Ortega, Y. Wakayama, D. Pena, *ACS Nano*, 2016, **10**, 9000. P. Ruffieux, S. Wang, B. Yang; C. Sanchez-Sanchez, J. Liu, T. Dienel, L. Tarliz, P. Shinde, C. A. Pignedoli, D. Passerone, T. Dumslaff, X. Feng, K. Mullen, R. Fasel, *Natur*e, 2016, **531**, 489 ; J. Cai, C. A. Pignedoli, L. Talirz, P. Ruffieux, H. Söde, L. Liang, V. Meunier, R. Berger, R. Li, X. Feng, K. Mullen, R. Fasel, *Nature Nano.,* 2015, **9**, 896; P. Ruffieux, J. Cai, N. C. Plumb, L. Pathey, D. Prezzi, A. Ferretti, E. Molinari, X. Feng, K. Mullen, C. A. Pignedoli, R. Fasel, *ACS Nano*, 2012, **6**, 6930.

3 C. Moreno, M. Vilas-Varela, B. Kretz, A. Garcia-Lekue, M. Costache, M. Paradinas, M. Panighel, G. Ceballos, S. O. Valenzuela, D. Pena, A. Mugarza, *Science*, 2018, **360**, 199; S. Kawai, S. Nakatsuka, T. Hatakeyama, R. Pawlak, T. Meier, J. Tracey, E. Meyer, A. S. Foster, *Sci. Advances* 2018, **4**, eaar7181; Z. Chen, H. I. Wang, N. Bilbao, J. Teyssandier, T. Prechtl, N. Cavani, A. Tries, R. Biagi, V. de Renzi, X. Feng, M. Klau, S. De Feyter, M. Bonn, A. Narita, K. Mullen, *J. Am. Chem. Soc.* 2017, **139**, 9483.

4 Z. Chen, A. Narita, K. Mullen, *Adv. Mater.,* 2020, **32**, 2001893; L. Tarliz, P. Ruffieux, R. Fasel, *Adv. Mater.,* 2016, **28**, 6222.

5 C. Sanchez-Sanchez, T. Dienel, O. Deniz, P. Ruffieux, R. Berger, X. Feng, K. Mullen, R. Fasel, *ACS Nano*, 2016, **10**, 8006; P. Han, K. Akagi, F. Federici Canova, R. Shimizu, H. Oguchi, S. Shiraki, P. S. Weiss, N. Asao, T. Hitosugi, *ACS Nano*, 2015, **9**, 12035; K. A. Simonov, N. A. Vinogradov, A. S. Vinogradov, A. V. Generalov, E. M. Zagrebina, N. Mårtensson, A. A. Cafolla, T. Carpy, J. P. Cunniffe, A. B. Preobrajenski, *J. Phys. Chem. C*, 2014, **118**, 12532.

6 F. Schulz, P. H. Jacobse, F. F. Canova, J. van der Lit, D. Z. Gao, A. von den Hoogenband, P. Han, R. J. M. Kelin Gebbink, M.-E. Moret, P. M. Joensuu, I. Swart, P. Liljeroth, *J. Phys. Chem. C*, 2017, **121**, 2896.

7 P. Han, K. Akagi, F. F. Canova, H. Mutoh, S. Shiraki, K. Iwaya, P. Weiss, N. Asao, T. Hitosugi, *ACS Nano*, 2014, **8**, 9181; K.A .A Simonov, N. A. Vinogradov, S. A. Vinogradov, A. V. Generalov, E. M. Zagrebina, N. Martensson, A. A. Cafolla, T. Carpy, J. P. Cunniffe, A. B. Preobrajenski, *ACS Nano*, 2015, **9**, 3399; P. Han, K. Akagi, F. F. Canova, H. Mutoh, S. Shiraki, K. Iwaya, P. Weiss, N. Asao, T. Hitosugi, *ACS Nano*, 2015, **9**, 3404.

8 S. Clair, D. G. de Oteyza, *Chem. Rev.*, 2019, **119**, 4717; Y. Makoudi, J. Jeannoutot, F. Palmino, F. Cherioux, G. Copie, C. Krzeminski, F. Cléri and B. Grandidier, *Surf. Sci. Rep.*, 2017, **72**, 316.

9 J. March in "*Advanced Organic Chemistry, 4th Edition*", Eds John Wiley& Sons, New York, 1992, p. 44.

10 E. A. Mader, E. R. Davidson, J. M. Mayer, *J. Am. Chem. Soc.* 2007, **129**, 5153.

11 C. Moreno, M. Panighel, M. Vilas-Varela, G. Sauthier, M. Tenorio, G. Ceballos, D. Pena, A. Mugarza, *Chem. Mater.*, 2019, *31*, 331.